INSPECTION OF BORON ANTIMONIDE THIN FILM DEPOSITED BY PULSED LASER DEPOSITION PROCESS THROUGH COMPLEX IMPEDANCE SPECTROSCOPY STUDIES

Dr. Shirsendu Das
Assistant Professor
Department of Physics
Uluberia College, Uluberia, Howrah,
West Bengal, India -711315

Email: shirsendudas4@gmail.com

Article History: **Received:** 18/03/2022 **Revised:** 16/05/2022 **Accepted:** 22/06/2022

Abstract:

Thin films of Boron antimode (BSb) have been successfully deposited on FTO coated glass substrate by PLDtechnique at 673K. The band gap was calculated to be ~0.55eV. Dielectric constant and dielectric loss factor were investigated with frequencies at various temperatures. The dielectric constant showed various natures arising due to the defects, impurities and space charge formation at the interface layers. The maximum dielectric loss was recorded at an applied a.c. frequency equal to the hopping frequency of the electrons, we obtained maximum dielectric loss factor. The energy per unit volume per unit time was calculated from the dielectric loss factor. Cole-Cole plots indicated two semi-circles in the high temperature domain (150K - 250K) while those measured in the lower temperature domain (10K - 125K) indicated one semicircle.

***Keywords*:** BSb; Boron Antimonide; Impedance; Dielectric Constant; Dielectric Loss

DOI: 10.53555/ecb/2022.11.6.34

1. Introduction:

The huge demand of finding alternate sources of energy has made the development of highly efficient solar cells demanding. Hot-carrier solar cells (HCSCs), which offer greater conversion efficiencies, are one of the main alternatives to the non-renewable energy sources. In this context the binary compounds like BSb perhaps has the greatest potential.[1]

For the above reasons, BSb has become a promising material platform for hot carrier absorber (HCA). Despite the advances of theories on BSb, the successful synthesis techniques of the compound were less reported. In our previous publication, we have discussed about the inherent difficulties in the synthesis procedure and achieved by the pulsed laser deposition process, the successful synthesis of BSb thin film with exact molar ratio.[2]The importance of study the temperature dependence of the complex impedance lies in understanding of the material and the mechanism involved in the electron conduction with respect to applications in HCSC. Amorphous $B_{12}Sb_2$ was first grown by molecular flow physical vapour deposition technique. The high mobility of $100cm^2/V$ s and high thermoelectric constant value of $10^{-4}/K$ observed by them revealed $B_{12}Sb_2$ a promising candidate for device fabrication.[3] In another report, the BSb films were synthesized by co-evaporation method. They explored the temperature dependent (210K - 360K) electrical conductivity of the films. However, they did not show the exact molar ratio of boron and antimony. [4]

Researchers should modulate the phononic band gap of the absorber material during the fabrication of HCSC. The localized density of states impedthe thermalization of the material in nanocrystalline form. As a result, in the tandem cells, the hot electrons are extracted maintaining their position for their constructive implementation of conversion of energy. [5]The electrical polarization under very low a.c. bias voltage with different temperature provides us very useful information related to the electron transport process in the hopping region in any disorder material. In our previous study, we demonstrated for the first time the possible electron transport procedure for the material BSb with theinvestigation of a.c. conductivity in a long temperature range (10K – 275K). Temperature independent conductivity was observed from 10K to 75K indicating insulating behaviour of BSb, Metal insulator transition around was observed at 75K. Beyond 75K the a.c. conductivity was decreased up to 125K like metal and after 125K the conductivity increased sharply showing semiconductor nature. The electron conduction of BSb was regulated by the thermal activation in the whole temperature range.[6] However, the complex electrical impedance properties of BSb thin film has not been explored till now by any researchers. This would give a clear picture on the density of states modulating the electron transport processes in these films especially in the sub-band gap region. Here, we have reported our measurements on the complex electrical impedance properties within a suitable range of temperature (10K -275K) and frequency (50 Hz-100 kHz).

2. Experimental Procedure:

We grew the boron antimonide thin films on FTO coated glass through PLD technique. The details of the technique have been described in detail elsewhere.[2] The films were deposited on to the substrates kept at 673K under identical deposition conditions indicated in reference[2]. The film thickness was ~500 nm. We examined surface morphology of the films by FESEM (Carl Zeiss AURIGA system). HIOKI-3532-50 impedance analyzer was employed during impedance measurements in the frequency range of 50 Hz to 100 kHz under the controlled temperature (10K - 275K). The temperature variation was achieved using a liquid helium cryostat and Lakeshore temperature controller.

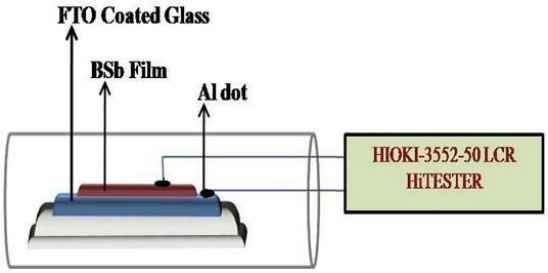

Figure 1: Schematic diagram of closed vacuum chamber for measurement of temperature dependent impedance spectroscopy.

Proper electrode configuration is crucial for recording the data for electrical conductivity of a thin film. We thermally deposited aluminum dots of diameter 1 mm on the BSb thin film as top electrode using proper mask under a vacuum pressure 10^{-6} Torr. FTO acted as bottom electrode during measurement. An a.c. voltage of 3mV was biased onto the sample during the dielectric polarization measurement. We mounted the sample on the cold finger into a helium cryostat and measured the impedance using several top

electrode dots on the BSb film (Fig.1). The results were consistence (varied within ±2%).

3. Results and discussion:

3.1. Microstructural and band gap studies:

Fig.2a portrays the electron microscopy images of BSb thin film. The FESEM picture shows distinct grains in the sample. Agglomeration of grains can also be observed along with some secondary nucleation sites. The histogram (inset of Fig.2a) shows a wide distribution of grain sizes ranging from 5 nm to 10 nm.

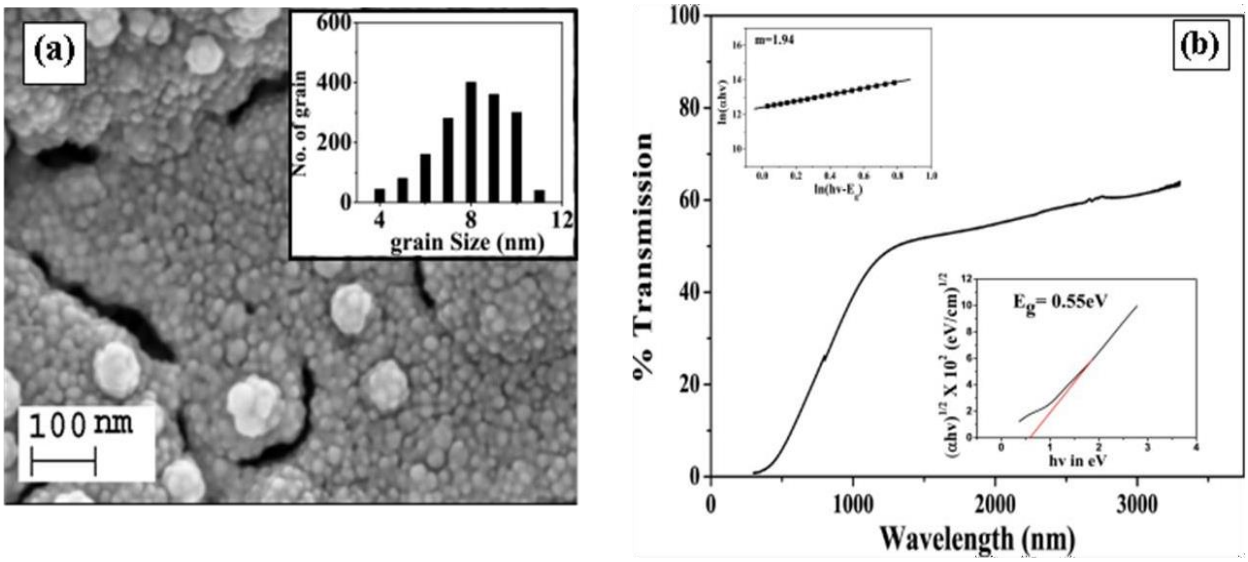

Figure 2: (a) FESEM picture of BSb film deposited at temperature 673 K and (b) Transmittance spectra of the BSb film. Top inset and bottom inset show the plot of ln ($\alpha h\nu$) versus ln ($h\nu$- E_g) and the plot of $(\alpha h\nu)^{0.5}$ versus $h\nu$ respectively.

Fig. 2b shows the transmission spectra of the same sample recorded in the wavelength range 300 nm to 3200 nm. The good crystal structure of the sample led a sharp trip at the band gap region of transmittance spectra. The absorption coefficient has been calculated with the help of the formula:[7, 8]

$$\alpha = \frac{A}{h\nu}(h\nu - E_g)^m \qquad (1)$$

The value of A and m depend on the nature of transition ('direct or indirect'). When hν is equal to E_g, the plot of d[ln(αhν)]/d[hν] with respect to hν diverges. This diverged point gives us abroad estimation of E_g. The value of m is calculated from the slope of the plot of ln(αhν) versus ln(hν-E_g) putting the rough estimated value of E_g(top inset of Fig.2b). Then the band gap can be calculated as shown in the bottom inset of Fig. 2b. Wecalculated the band gap as 0.55 eV for indirect transition. The band gap value obtained by us matched well with the predicted value by density functional theory.[9]

3.2. Impedance spectroscopy:

The inter-dependency of the electrical properties on micro-structure of a material can be explored with the help of the complex impedance spectroscopy (CIS). The electrical properties along with the electrochemical features of polycrystalline material can be characterized through CIS technique. There is a very close relation between the electrical response and microstructure.

3.2.1 Complex Impedance Studies:

Conventionally, the impedance data are exhibited in a complex plane. Involvement of various mechanisms related to a.c. conduction and polarization relaxation can be explained bystudying the impedance over a frequency range. We can clearly separate the contribution of bulk, grain boundaries and interfaces separately fromthe graph depicted the variation of impedance with frequency. In case of polycrystalline material, the impedance and capacitance arise due to the existence of inter-granular/ grain boundary. Different values of resistivity and dielectric constant can be observed for a material consisted of grain and grain boundaries, both. Impedance data are presented in the form of imaginary, *Z''*(capacitive) against real, *Z'* (resistive) impedances.[10]

Fig.3a and Fig.3b show the variation of real portion of impedance (Z′) with frequency at various temperatures from 10K to 125K and from

150K to 275K, respectively. One may observe (Fig.3a) that the real portions of impedance (Z′) are nearly frequency independent up to ~1.5kHz and after that Z′ started increasing with frequency.

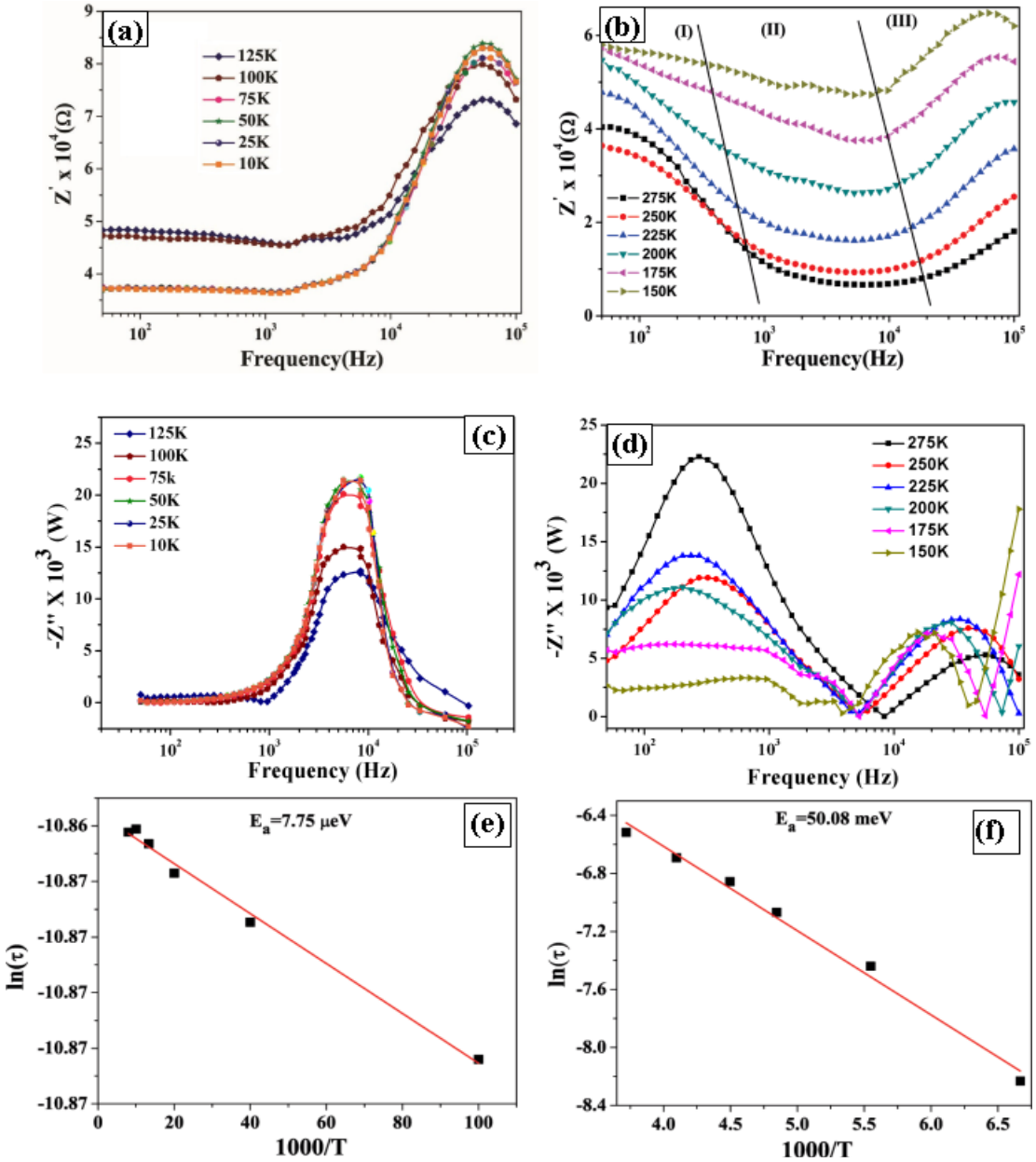

Fig. 3: Variation of Z′ with frequencies when the temperature was varied: (a) from 10K to 125K and (b) from 150K to 275K. Variation of Z′′ with frequencies when the temperature was swept: (d) from 10K to 125K and (d) from 150K to 275K. Plots of ln (τ) vs. 1000/T: (e) at temperature 10K to 125K and (f) at temperature range 150K to 275K.

Z′ attains maximum at ~5.5x10^{4}Hz. In this temperature range (10K to 125K), the conductivity initially appears frequency independent, increases in the mid frequency range and later, decreases at higher frequencies (Fig.3a). The above frequency independent region indicates purely resistive part of the sample. The dispersive region signifies the reactive part of the sample. In the temperature range of study, Z ′remained quite invariant with temperature in the plateau region and started decreasing with increment in temperature after the plateau region. The values of Z′ nearly overlapped with one another in the higher frequency region at all temperatures (10K to 125K). The elevation in conduction due to the space charge release with increase of temperature at high frequencies causes this above discussed variation.

The behaviour of Z ′at a broad frequency range in the temperature range 150K - 275K is shown in Fig.3b. The free movement of released space charge lowers the energy barrier, which causes the

decrease in Z' when the temperature stays in between 150K to 275K (Fig.3b).[11-13] This is totally different from the previous one. The values of Z' decreased with temperature. The behaviour of Z' shows a decreasing trend with frequency (region-I) followed by an almost frequency independent plateau (region-II) and again increasing with frequency (region-III).

Fig.3c and Fig.3d depict the trend of complex impedance (Z'') with frequencies in two different temperature domains of 10K-125 K and 150 K - 275K, respectively. In Fig.3c one may observe that the frequency independent trend of Z'' upto ~1kHz. No significant variation except the peak height was observed with temperature. Beyond 1kHz, Z'' increased sharply with frequency reaching a peak value at ~$8x10^3$ Hz. It decreased again due to the existence of relaxation phenomena. The accumulation of space charge in the material leads merging the values of Z'' for all temperatures at high frequencies. [14]The existence of relaxation properties could be ascribed to the appearance of peaks. The appearance of immobile ions/electrons and defect or vacancy states cause the relaxation peaks at low and high temperature, respectively, at the particular a.c. biased frequency when it is equal to the localized electrons, hopping frequency. Spread of the relaxation time would culminate in lack of symmetry in the peak broadening. The peak value of maxima of Z'' versus frequency plots also decreased with the increase in temperature (Fig.3c). Slight broadening of Z'' peaks was observed with the increase in temperature due to thermal relaxation process. The immobile ions and the defects results the above relaxation at lower temperatures and higher-temperature, respectively.[15] The variations of Z'' with frequencies in the temperature range 150K-275K are indicated in Fig.3d. This variation is much more complex than that has been observed in the lower temperature (10K -125K) region (Fig.3c). Shift of the peak position towards higher frequency indicates decrease in relaxation time with the increase of temperature. [12] The observed peak broadening with increasing temperature would suggest that the electrical relaxation phenomenon in this material depends on temperature. [16] The relaxation process may be ascribed to the existence of space charges and mobility of the above space charges is increasing with increasing temperature.

A significant broadening of peaks with temperature indicates the appearance of temperature dependent relaxation process in the materials. [17]We already have discussed the role of electrons, immobile ions and defect states in relaxation process in different temperature regions. The relaxation time (τ) is determined from the peak of Z'' versus frequency plot (Fig.3e and 3f) following the relation $2\pi f_r r = 1$ where f_r is the relaxation frequency. It is note worthy to mention that this peak position does not depend on the geometrical parameters of the sample during measurement. The linear dependency of τ with $10^3/T$ which can be fitted through an equation $\tau = \tau_o \exp(-E_a/k_B T)$ where τ_0, E_a and k_B are the pre - exponential factor, the activation energy and the Boltzmann constant, respectively.[18] Figs.3e and 3f portray the dependency of relaxation time with inverse of temperature. The calculated activation energies of BSb are 7.75 eV in the temperature range 10 K - 125K (Fig. 3e) and 50.08 meV in the temperature range 150 K -275K (Fig. 3f). This value matches well with that obtained from a.c. conductivity measurement. [6]

3.2.2 Dielectric constant and dielectric loss factor:

The complex dielectric permittivity is given by therelation: [19]

$$\varepsilon = \varepsilon' - j\varepsilon'' \qquad (2)$$

where, ε' and ε'' are the dielectric constant of the material and dielectric loss factor, respectively. Dielectric constant of the material (ε') and dielectric loss factor (ε'') were measured as a function of frequencies at different temperature ranging from 10K to 275K. Fig.4a and Fig.4b depict the variation of ε' and ε'' with frequencies at various temperatures (10K -275K),respectively. It may be observed (Fig.4a) that the dielectric constant (ε') dropped down when frequency increased. Values of both dielectric constant and loss factor were higher at higher temperature especially in the decreased frequency ranges. One may see that ε' and ε'' measured at lower temperatures is nearly invariant with frequency in this system. The large number of charge accumulation at the interface of electrode and sample could lead the deviation. In the high frequency region, ε'drops down due to the fast repetitive switching speed of applied filed at particular interface. The high speed of changing biased field reduces the contribution from the charge carriers to the dielectric constant. [20]

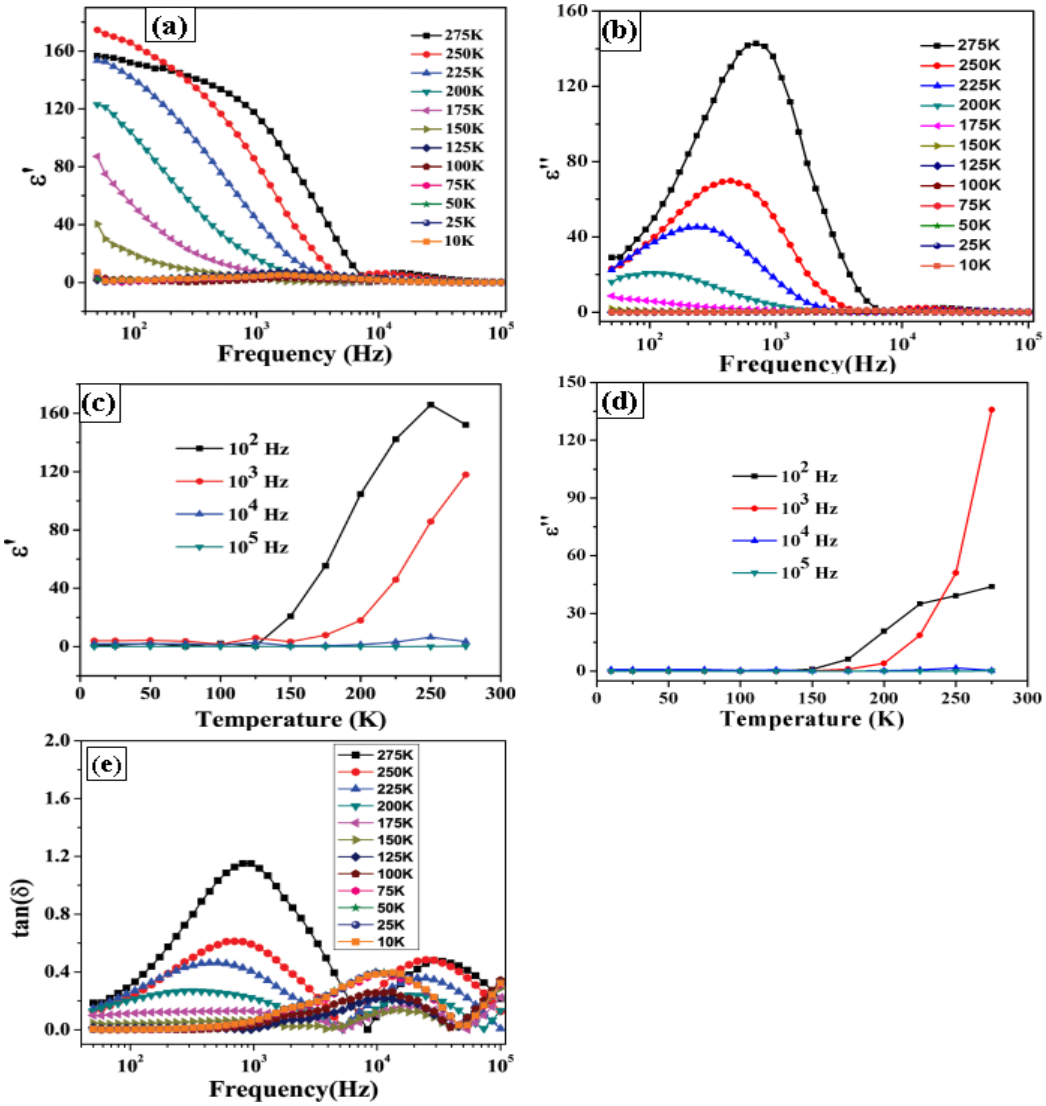

Figure 4: Variation of (a) dielectric constant (ε′) and (b) loss factor (ε′′) with frequencies when the temperature range varies from 10 K to 275K. Variation of (c) ε′ and (d) ε′′ with different temperaturesat particular frequencies of 10^2 Hz, 10^3 Hz, 10^4 Hz and 10^5 Hz. (e) tan (δ) with frequencies in the temperature range 10-275K.

Variation of dielectric loss factor (ε'') with frequencies is depicted in Fig.4b. In a.c. fields, the energy loss (W) per unit volume per unit time may be calculated from the equation: [21]

$$W = \frac{\omega s_0 E^2}{8\pi} \varepsilon'' \qquad (3)$$

W values, computed using eqn.3 and ε'' value as shown in Fig.4b, are shown in Table-1.

Table-1: Energy loss W at frequencies 1 kHz and 10 kHz in the temperatures 10K, 100K, 200K and 275K

Temperature (K)	Energy loss (Watt)	
	At 1kHz	At 10kHz
10	19.61	60.33
100	4.15	24.05
200	335.63	16.23
275	11422.05	25.59

At all temperatures, one may observe that energy loss is invariant when the frequency domain is higher. But loss is significantly higher at lower frequency domain especially in the higher temperature region. This is basically due to the defects, impurities and space charge generation at the interface layers which would induce an absorption current causing dielectric loss in this granular material. More specifically, the property of interest may generally be related to the grain

boundaries in polycrystalline materials. Therefore, the more conducting grains and the comparatively less conducting grain boundaries regions acted as interfaces provide the dielectric structuretogether. Due to the applied electric field, this dielectric structure leads the accumulation of charges at the interface regions and results in interfacial polarization. In order to characterize the microstructures and electron transport properties of materials like BSb films under consideration, which consist of various resistive domains, impedance spectroscopy techniques would provide the required provisions that would probe the different regions according to their electrical relaxation times or time constants.

The appearance of peaks with different intensities in dielectric loss factor (ε'') especially at higher temperatures may be due to the presence of various relaxation processes induced at different temperature. Origin of different relaxation processes is generally for the existence of defects, vacancies at higher temperatures. [16, 22] With increasing temperature, the dielectric loss increased and the peaks shift gradually towards higher frequency. The curves, then merge together in high frequency region. The conductivity in this granular material would mainly be governed by hopping of electrons. [4] Dielectric behaviour of any sample is correlated with conductivity through hopping of electrons. With increasing temperature, the probability of hopping of the electrons per unit time would increase culminatingin an increase in loss factor. When the frequencyof the applied a.c. field equals the hopping frequency, one would expect a maximum loss factor. At higher frequencies, the loss factor would be reduced due to the low value of absorption current. [23] The loss factor is mainly due to the vibration of the lattices (phonons) at high frequency region. [24]

Fig.4c and Fig.4d show the temperature dependence of ε' and ε'' with temperature for four different frequencies (100 Hz, 1 kHz, 10 kHz, 100 kHz), respectively. The values of dielectric constant (ε') start increasing with temperatures at and above 125K. The temperature dependence of the dielectric constant (ε') was found to be less pronounced in the higher frequency domain. The rate of increment ofε' with temperature is significantly higher at 100Hz-1kHz region than 10kHz-100kHz region. Disorder in cation sublattices would arise from shifting of a cation from one side to another which may cause this kind nature of variation. The increase in ε' would weaken the coulomb interaction between cations. Due to this type of weak interaction, the cations would jump to another unit cell creating a vacancy behind. This may be the possible reason of shift from a state of low dielectric constant (ε') in an ordered cation sublattice to a state of high dielectric constant (ε') in a disordered cation sublattice with increasing temperature. [25]Two components: the capacitive (I_C) and the resistive (I_R) coming from impurities, dirt, moisture etc. comprise the total current component in a capacitor during current flow. The impurities cause the developments of conductive paths through insulating regions. Conventionally, the capacitive current (I_C) leads the applied voltage by a phase difference of 90° and the resistive current continues same phase with the applied voltage. Therefore, we define the ratio (I_R/I_C) as tan (δ) or dissipation factor. The Fig.4e demonstrates the behaviour of dissipation factor with frequencies in all temperatures. We recorded low magnitudes of dissipation factor. From this observation we conclude the greater presence of the capacitive current component over the resistive one. Thus, wecan say this material provides a good capacitive path during A.C. conduction.

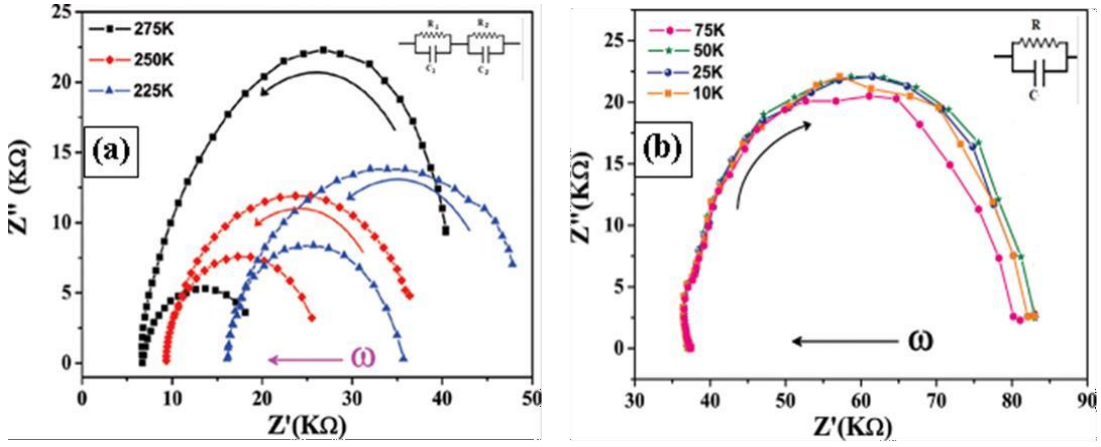

Fig. 5: Cole-Cole plot (Z′′vsZ′) in different temperatures:(a) at 225K, 250K, 275K and (b) at 10K,25K, 50K, 75K.

Fig.5a and Fig.5b show the Cole-Cole plots of the BSb system under study for two temperature domains: 225K-275K and 10K -75K, respectively. In the high temperature region 225K to 275 K, the Cole-Cole plots indicated two semi- circles (Fig.5a) while those measured in the low temperature domain (10K -75K) (Fig. 5b) indicated one semicircle. At higher temperature domain, the BSb films behaved like a typical semiconductor whose electron transport phenomenon was mainly controlled by Mott's hopping.[26, 27] The semicircle with larger radius would contain information on granular BSb film in the semiconducting domain. The contributions of bulk and interface in impedance result the semicircular arcs separately in high and low frequency regions, respectively(Fig.5a).[10]As BSb shows semiconducting property in the high temperature region, so when we increased temperature the resistance decreased which led to the shortening the diameters of semicircular arcs. The point where the semicircular arc met the real axis moved toward the origin point of the graph with increment of temperature due to the low resistance of the BSb compound. The difference in diameters of the semicircles could be seen to decrease as the measurements are carried out at lower temperatures (Fig.5a). One single semicircle was obtained when the measurements were carried out at relatively lower temperatures (Fig.5b). The corresponding second short semicircle (Fig.5a) in the lower frequency region may represent the contact effect arising out of top aluminium and/or bottom FTO contact to the BSb material. The radius of the short semicircle gradually increased and tended to merge with the larger one and ultimately became indistinguishable at lower temperature (Fig.5b).It has been observed here that the BSb films would behave like an insulator and in the low temperature domain (10 K -125 K), the electron transport phenomenon would likely be controlled by Efros-Shklovskii model for hopping within the Coulomb gap.[6, 28-30]The collapsing of the Coulomb gap was happened, as the critical point for the transition was reached as described by Pollak and Zabordskii et al.[31-33]The electrical conductivity was nearly invariant at temperature 10 K to 75 K for all frequencies. This is a typical characteristic of variable range hopping (VRH) in the low temperature regime. The presence of one semicircle in the Cole-Cole plot in the lower temperature domain would be represented by nearly similar semicircles for all the measurements carried out in the lower temperature domain. The departure from the low resistance state to the high resistance state culminates in significant increase in the bulk impedance. The interface impedance then increases simultaneously. The difference in the interface component would over shadow the effect associated in the bulk component. This single semicircular arc would be due to the predominant high resistance state of the samples at lower temperatures. Single semi- circular arc generally reflects the dominant influence of the bulk conduction in BSb and has been expressed by an equivalent parallel R–C circuit (Fig. 5b). The combined influence of grain and grain boundaries in impedance are modeled through an equivalent circuit containing series connection of two parallel R-C circuits due to the presence of two semicircular arcs in Cole-Cole plot, as shown in (Fig. 5a).

4. Conclusion:

BSb film, deposited successfully through PLD technique at 673K reported a band gap of ~ 0.55eV for indirect transitions. The low temperature impedance behaviour of BSb has been investigated for the first time. Two types of impedance (Z') properties were observed with frequency at various temperatures from 10K to 125K and from 150K to 275K. Dielectric constant of the material (ε') and dielectric loss factor (ε'') were measured with frequencies in various temperatures. The dielectric constant shows various types of nature due to the defects, impurities and space charge formation in the interface layers in sublattices. Maximum dielectric loss factor (ε'') was achieved when the applied a.c. frequency was equal to the hopping frequency of the electrons. The energy per unit volume per unit time was calculated from the dielectric loss factor. This study indicated maximum loss at 1kHz at 200K and 275K. Cole-Cole plots indicated two semi-circles when measured in the high temperature domain (150-250 K) while those measured in the lower temperature domain (10-125 K) indicated one semicircle. We can firmly say that our study will help the researchers devoted to the materials studies related to solar cell and other electronic application to get a clear idea of electrical polarization behaviour under a small a.c. bias from in low temperature range.

Acknowledgements:

The authors express their warm gratitude to the UGC-DAE CSR, Government of India and Board of Research in Nuclear Sciences (BRNS), Government of India for the financial support for the completion of the research work.

References:

1. Y. Yao, D. König, M. Green, Investigation of boron antimonide as hot carrier absorber material, Solar Energy Materials and Solar Cells, 111 (2013) 123-126.
2. S. Das, R. Bhunia, S. Hussain, R. Bhar, B.R. Chakraborty, A.K. Pal, Synthesis and characterization of boron antimonide films by pulsed laser deposition technique, Applied Surface Science, 353 (2015) 439-448.
3. Y. Kumashiro, K. Nakamura, K. Sato, M. Ohtsuka, Y. Ohishi, M. Nakano, Y. Doi, The properties of B–Sb thin films prepared by molecular flow region PVD process, Journal of Solid State Chemistry, 177 (2004) 533-536.
4. S. Dalui, S.N. Das, S. Hussain, D. Paramanik, S. Verma, A.K. Pal, BSb films: Synthesis and characterization, Journal of Crystal Growth, 305 (2007) 149-155.
5. D. König, K. Casalenuovo, Y. Takeda, G. Conibeer, J.F. Guillemoles, R. Patterson, L.M. Huang, M.A. Green, Hot carrier solar cells: Principles, materials and design, Physica E: Low-dimensional Systems and Nanostructures, 42 (2010) 2862-2866.
6. S. Das, R. Bhunia, S. Hussain, R. Bhar, A. Kumar Pal, Alternate current conductivity in BSb films prepared by PLD technique: Electron transport processes in low-temperature range (10-275 K), The European Physical Journal Plus, 132 (2017) 176.
7. J.C. Manifacier, J. Gasiot, J.P. Fillard, A simple method for the determination of the optical constants n, k and the thickness of a weakly absorbing thin film, Journal of Physics E: Scientific Instruments, 9 (1976) 1002-1004.
8. D. Bhattacharyya, S. Chaudhuri, A.K. Pal, Bandgap and optical transitions in thin films from reflectance measurements, Vacuum, 43 (1992) 313-316.
9. A. Zaoui, S. Kacimi, A. Yakoubi, B. Abbar, B. Bouhafs, Optical properties of BP, BAs and BSb compounds under hydrostatic pressure, Physica B: Condensed Matter, 367 (2005) 195-204.
10. J.T.S. Irvine, D.C. Sinclair, A.R. West, Electroceramics: Characterization by Impedance Spectroscopy, Advanced Materials, 2 (1990) 132-138.
11. A. Kumar, B.P. Singh, R.N.P. Choudhary, A.K. Thakur, Characterization of electrical properties of Pb-modified BaSnO3 using impedance spectroscopy, Materials Chemistry and Physics, 99 (2006) 150-159.
12. B. Behera, P. Nayak, R.N.P. Choudhary, Impedance spectroscopy study of NaBa2V5O15 ceramic, Journal of Alloys and Compounds, 436 (2007) 226-232.
13. J. Płcharski, W. Weiczorek, PEO based composite solid electrolyte containing nasicon, Solid State Ionics, 28-30 (1988) 979-982.
14. A. Dutta, C. Bharti, T.P. Sinha, Dielectric relaxation in Sr(Mg1/3Nb2/3)O3, Physica B: Condensed Matter, 403 (2008) 3389-3393.
15. W. Lu, S. Jiang, D. Zhou, S. Gong, Structural and electrical properties of Ba(Sn,Sb)O3 electroceramics materials, Sensors and Actuators A: Physical, 80 (2000) 35-37.
16. B. Behera, P. Nayak, R.N.P. Choudhary, Structural and impedance properties of KBa2V5O15 ceramics, Materials Research Bulletin, 43 (2008) 401-410.
17. A.K. Jonscher, The 'universal' dielectric response, Nature, 267 (1977) 673-679.
18. S. Dutta, S. Bhattacharya, D.C. Agrawal, Electrical properties of ZrO2–Gd2O3 ceramics, Materials Science and Engineering: B, 100 (2003) 191-198.
19. P.B. Macedo, C.T. Moynihan, R. Bose, ROLE OF IONIC DIFFUSION IN POLARIZATION IN VITREOUS IONIC CONDUCTORS, Physics and Chemistry of Glasses, 13 (1972) 171-179.
20. J.R. Macdonald, Impedance spectroscopy, Annals of Biomedical Engineering, 20 (1992) 289-305.
21. M.S. Aziz, Y.A. Aggour, Electrical conduction of polymer complexes of 2-(dimethylamino)ethyl acrylate with cobalt chloride, Polymer Testing, 18 (1999) 511-521.
22. H. Singh, A. Kumar, K.L. Yadav, Structural, dielectric, magnetic, magnetodielectric and impedance spectroscopic studies of multiferroic BiFeO3–BaTiO3 ceramics, Materials Science and Engineering: B, 176 (2011) 540-547.
23. B. Behera, P. Nayak, R.N.P. Choudhary, Study of complex impedance spectroscopic properties of LiBa2Nb5O15 ceramics, Materials Chemistry and Physics, 106 (2007) 193-197.
24. J. Hassan, F.M. Yen, M. Hashim, Z. Abbas, Z. Abdul Wahab, W.M.D. W. Yusoff, A. Zakaria, Dielectric permittivity of nickel ferrites at microwave frequencies 1 MHz to 1.8 GHz, Ionics, 13 (2007) 219-222.
25. T. Kar, R.N.P. Choudhary, Structural dielectric and electrical conducting properties of KB′B″O6 (B′=Nb, Ta; B″=W, Mo) ceramics, Journal of Physics and Chemistry of Solids, 62 (2001) 1149-1161.

26. N.F. Mott, Conduction in non-crystalline materials, The Philosophical Magazine: A Journal of Theoretical Experimental and Applied Physics, 19 (1969) 835-852.
27. N.F. Mott, E.A. Davis, Electronic processes in non-crystalline materials, Oxford university press2012.
28. M.R. Graham, J.R. Bellingham, C.J. Adkins, Hopping conduction near the metal-insulator transition in amorphous indium oxide, Philosophical Magazine B, 65 (1992) 669-673.
29. A.L. Efros, B.I. Shklovskii, Coulomb gap and low temperature conductivity of disordered systems, Journal of Physics C: Solid State Physics, 8 (1975) L49-L51.
30. C.J. Adkins, Conduction in granular metals-variable-range hopping in a Coulomb gap?, Journal of Physics: Condensed Matter, 1 (1989) 1253-1259.
31. M. Pollak, The Coulomb gap: A review, and new developments, Philosophical Magazine B, 65 (1992) 657-667.
32. A.G. Zabrodskii, The Coulomb gap: The view of an experimenter, Philosophical Magazine B, 81 (2001) 1131-1151.
33. A.G. Zabrodskii, A.G. Andreev, S.V. Egorov, Coulomb Gap and the Metal–Insulator Transition, physica status solidi (b), 205 (1998) 61-68.